Journal of Colloid and Interface Science 581 (2021) 682–689

Contents lists available at ScienceDirect

Journal of Colloid and Interface Science

journal homepage: www.elsevier.com/locate/jcis

The effect of alginate composition on adsorption to calcium carbonate surfaces

Kathryn Louise Browning [a,b,*], Isabella N. Stocker [a,c], Philipp Gutfreund [d], Stuart Matthew Clarke [a]

[a] BP Institute, University of Cambridge, Cambridge, UK
[b] Department of Pharmacy, University of Copenhagen, Copenhagen, Denmark
[c] BP Exploration Operation Company Ltd., Sunbury-on-Thames, UK
[d] Institut Laue-Langevin, Grenoble, France

HIGHLIGHTS

- Sodium alginate adsorption to calcite in water was studied using neutron reflection.
- Alginate formed highly hydrated layers at the surface with Gaussian distribution.
- Alginates with high guluronic acid adsorbed more than with high mannuronic acid.
- High guluronate alginates roughened the surface more due to complexation of calcium.
- Added magnesium ions caused lower roughening and adsorption of alginate to calcite.

GRAPHICAL ABSTRACT

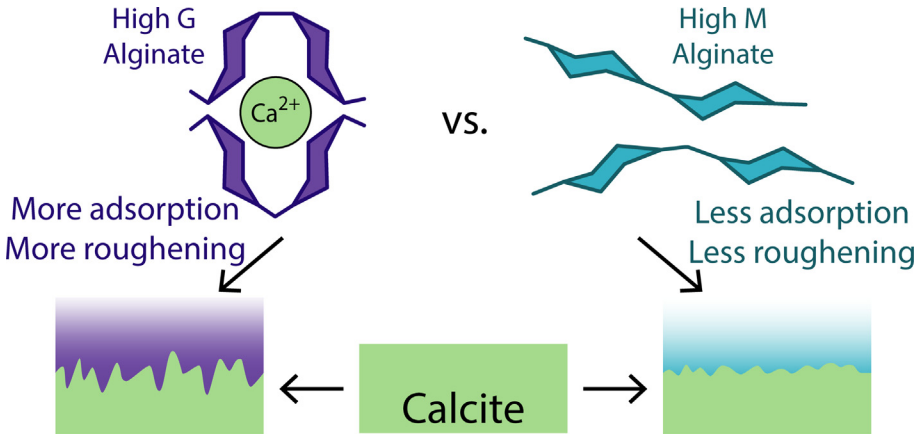

ARTICLE INFO

Article history:
Received 27 May 2020
Revised 9 July 2020
Accepted 17 July 2020
Available online 22 July 2020

Keywords:
Calcium carbonate
Calcite
Polysaccharides
Alginate
Biomineralization
Mannuronic acid
Guluronic Acid
Adsorption
Neutron reflection
Interfaces

ABSTRACT

Bacterial anchoring to limestone rocks is thought to occur by selective adsorption of biomolecules found in the extracellular matrix, such as polysaccharides. Here we study the adsorbed structure of a model matrix polysaccharide, sodium alginate, at the calcite/water interface using neutron reflection (NR). Sodium alginate was found to form highly hydrated layers extending up to 350 Å into solution at concentrations up to 2.5 ppm (the inflection point of the adsorption isotherm). The adsorption of alginate was driven by dissolution of the calcite surface through complexation of free calcium ions. This was shown using two alginates with differing ratios of sugar residues. Alginates with a higher proportion of guluronic acid (G) have a higher affinity for calcium ions and were found to cause the surface to dissolve to a greater extent and to adsorb more at the surface when compared to alginates with a higher proportion of mannuronic acid (M). Adding magnesium to the high G alginate solution reduced dissolution of the surface and the adsorbed amount. In this work, we have shown that polysaccharide adsorption to sparingly soluble calcite interfaces is closely related to polymer conformation and affinity for free calcium ions in solution.

* Corresponding author at: Department of Pharmacy, University of Copenhagen, Universitetsparken 2, Copenhagen 2100, Denmark.
E-mail addresses: kathryn.browning@sund.ku.dk (K.L. Browning), isabella.stocker@cantab.net (I.N. Stocker), gutfreund@ill.fr (P. Gutfreund), stuart@bpi.cam.ac.uk (S.M. Clarke).

https://doi.org/10.1016/j.jcis.2020.07.088
0021-9797/

1. Introduction

Most of the Earth's calcite ($CaCO_3$) is of biogenic origin from carbonaceous marine organism sedimentation. Calcium carbonate biomineralisation provides structure throughout Nature from avian eggshells to marine molluscs and coccoliths [1,2]. The fine control of crystal morphology, phase and grain size is moderated through the production of various biomolecules, which also affect the mechanical properties [2,3]. The precise mechanism by which these molecules interact with the crystallizing medium through nucleation and growth is an area of current interest in several areas, including amorphous calcium carbonate precursor phases (ACC) [3–9].

Calcium carbonate can be precipitated in several different polymorphs of varying stability. The most stable polymorph under ambient conditions is calcite; it can form large defect-free crystals, making it suitable as the focus of this experimental study. It is sparingly soluble in water with a solubility product at room temperature of $K_{sp} = 3.7 \times 10^{-9}$ mol dm^{-3} [10]. This dissolution complicates the analysis of adsorption to calcite surfaces as acidic conditions can lead to a highly dynamic interface. The dissolution or precipitation of calcite is closely linked with other aqueous equilibria that determine the extent of dissolution of the surface [11].

The driving force for adsorption of polyanionic polysaccharides is expected to be the affinity of the charged carboxylate groups for calcium on the positively charged calcite surface. Calcium cations released from the calcite surface are sequestered to the sugar forming a complex. This process in turn removes calcium from the solution shifting the equilibrium such that more calcium carbonate solid is dissolved. Polyanionic polysaccharides have been shown to affect the crystal growth structure of calcium carbonate by interacting with the mineral surface suggesting specific interactions with the calcite surface [12]. Furthermore, negatively charged sugars secreted by bacteria into the extracellular matrix may aid anchoring of the cell to calcitic limestone rocks in marine environments [13,14].

Sodium alginate has been chosen for this study as a model polysaccharide due to its well-understood structural characteristics and calcium binding properties, allowing the interplay between complex-mediated surface dissolution and polymer adsorption to be investigated [15]. Alginates are a major structural component of marine algae and secreted by some bacteria, most notably *Pseudomonas aeruginosa* and *Azotobacter vinelandii* [16]. As schematically illustrated in Fig. 1, sodium alginate is a copolymer of two epimers, mannuronic acid (M) and guluronic acid (G), which differ only by the conformation of the 1,4 glycosidic link. The two sugar residues can be found either as homopolymeric blocks of each sugar or as alternating MG sequences [17]. The primary structure of alginate affects the macromolecular properties greatly. GG blocks are rigid as the axial linkage decreases movement and provides a binding site for divalent cations. Conversely, MM blocks are joined via an equatorial glycosidic linkage and therefore relatively free [17]. The molecular conformation of the pairs, MM, MG and GG are included in Fig. 1.

Two gram negative, alginate producing, bacteria, *Pseudomonas aeruginosa* and *Azotobacter vinelandii*, secrete alginates with different compositions, macromolecular properties, and functions. *P. aeruginosa* secretes alginate as a protective envelope and adhesive molecule in biofilm formation in the lung, these alginates have little to no G blocks [16]. Conversely, *A. vinelandii*, a soil bacterium that forms exopolysaccharide cysts in soil to protect from mechanical stress and desiccation during dormancy, produces alginates with high ratios of GG blocks and alternating sequences in the outer protective layer [16].

The more rigid GG sections provide well-defined chelation sites, which leads to gelation on addition of calcium. The more flexible MM and MG blocks deform to allow adjacent GG disaccharide units to line up form a chelating cage composed of four G saccharide units [18]. This ability to co-ordinate is strongly linked to conformational structure; alginates with a higher proportion of G (and G blocks) gel at lower concentrations of calcium ions and form stronger and more brittle gels [19,20]. Grant *et al.* defined this guluronate-Ca interaction the 'egg-box model' due to the alignment of guluronate chains along a plane of calcium ions [17,21]. In contrast to calcium, the binding of magnesium with alginate molecules is reported to be a non-specific interaction [22,23]. Magnesium alginate is soluble and does not strongly interact with any specific binding sites [23,24].

In this study we have used neutron reflection and bulk solution depletion isotherms to compare the adsorption of two different sodium alginate samples with either a low (MVM) or high (MVG) content of guluronate residues to calcium carbonate surfaces. Considering the higher affinity of guluronate residues to calcium ions in solution, the two alginates are expected to show very different surface adsorption profiles in terms of both adsorbed amount and structure. Neutron reflectivity allows the measurement of complex adsorbed structures at the solid/liquid interface, something which is challenging using other techniques. The study of the solid/liquid interface using neutron reflection has been reasonably limited to a small number of single crystal interfaces, mainly silicon, quartz and sapphire [25]. Recently the number of mineral surfaces used in reflection experiments has widened to include calcite, however, previous work has focused on the adsorption of industrial chemicals and surfactants at the calcite/liquid interface [26–28]. Here we aim to investigate the adsorption of biopolymers to calcite surfaces in aqueous environments to show how polymer conformation and calcium ion dissolution from the calcite surface can affect adsorbed amount and structure at the interface.

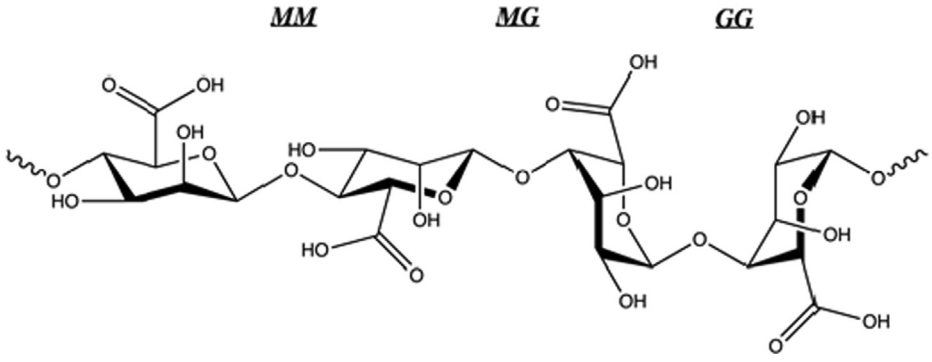

Fig. 1. Molecular structure of the alginic acid showing the various links between the two epimers, MM, MG and GG diblocks.

2. Experimental

2.1. Materials

All experiments were carried out using two ultrapure and well-characterised alginates (Pronova UP Test kit) obtained from Novamatrix. The two alginates tested were of medium viscosity (>200 mPa·s) and high molecular weight (>200 kDa) and only differ by the ratio of the two sugar epimers. The high guluronate sample (Medium Viscosity Guluronate, MVG) was reported to have a viscosity of 263 mPa·s and contain 69% guluronate residues. The high mannuronate sample (Medium Viscosity Mannuronate, MVM) was found to have a higher viscosity (553 mPa·s) with a mannuronic acid content of 54%. All values quoted here were obtained from the manufacturers certificate of analysis of the batch used.

Calcium carbonate powder (≥99%) used for adsorption isotherms and to saturate water for NR experiments was purchased from Sigma Aldrich. Calcite crystals used in neutron reflection experiments were optically clear Iceland Spar crystals obtained from P&E Export Ltd, Brazil. The large rhombohedral crystals were cut to a cuboid shape (40 × 55 × 15 mm) and polished to a low roughness by Crystran, Poole, UK. The surface for reflectivity was the most stable $\{10\bar{1}4\}$ face, the crystallographic plane found at the surface of the natural rhomb. Attempts were made to cleave the surface rather than polish, however, it was not possible to obtain an area large enough for reflectivity studies (roughly 20 cm^2) without introducing large steps, causing the cells to leak. The roughness of the polished crystals was assessed by X-ray reflectivity on a Rigaku SmartLab X-ray diffractometer (ISIS, Rutherford Appleton Laboratory, Didcot, UK). This measurement gave an approximate indication of the quality of the surface (data shown in supporting information, Fig. S1). Crystals with an X-ray roughness less than 15 Å were then used in neutron reflectivity experiments.

2.2. Adsorption isotherms

Isotherm measurements were carried out using a solution depletion batch method. 2 g of calcium carbonate powder was homogenised with 498 g ultrapure water using a Silverson L4R shear mixer for 10 min. The slurry was then weighed into centrifuge tubes and increasing amounts of alginate stock solution was added. The samples were agitated overnight and centrifuged at 15,000 G for 20 min. The supernatant was removed and filtered through a 0.45 μm polyethersulfone syringe filter (QMX, UK). The Total Organic Carbon content of the supernatant was measured using a GE InnovOx TOC Analyser. During analysis, the supernatant was acidified and purged with nitrogen to remove traces of inorganic carbonates. The concentration of non-purgeable carbon remaining in the supernatant was then used to calculate the adsorbed amount of alginate.

2.3. Neutron reflectivity

The experiment is performed by illuminating a large flat crystal with a collimated beam of neutrons, which reflect and/or refract at the solid/liquid interface. The intensity of the reflected beam is then measured as a function of wavelength and reflected angle. In this experiment, the D17 reflectometer at the Institut Laue-Langevin, France [29], was used in the time-of flight (TOF) mode where a polychromatic beam of neutrons is directed at the sample and the wavelength determined by the time taken for neutrons to reach the detector from the source. The determined wavelength values are converted to a momentum transfer vector, Q, calculated from equation (1).

$$Q = \frac{4\pi sin\theta}{\lambda} \quad (1)$$

The use of the TOF method on D17 allows the entire scattering range of interest of the reflectivity curve to be measured using only two incident angles, 0.6° and 2.0°, to cover a Q range of 0.006–0.2 $Å^{-1}$. To ensure no contribution from the edges of the sample, a constant beam footprint of 30 × 45 mm^2 was maintained on the sample surface. The dQ/Q resolution varied between 1.5 and 10% over the Q range measured, during data fitting a value of 4% resolution was used. The data reduction was performed using the COSMOS software [30].

The calcite crystals were cleaned by UV-Ozone treatment (Bio-Force Nano Procleaner). After irradiation, a small drop of filtered calcium carbonate saturated water was placed on the surface to assess wettability. If the droplet spread the crystal was considered clean, placed immediately against a Teflon trough, and sealed in a neutron reflectivity cell (details of cell reflection sample cell are given in Stocker *et. al.* [26]). Sample changes were carried out by draining the sample cell by pipette (3 mL cell volume) and refilling in-situ with the required solution, this process was repeated three times and the cell sealed with Teflon plugs.

2.4. Analysis of reflectivity data

The shape of the reflectivity curve at a single interface is determined by the surface roughness and the change in neutron refractive index upon moving from one medium to the next through the surface. Neutron reflection theory is outlined elsewhere [31]. A particularly powerful aspect of neutron reflection is the seemingly random nature of neutron scattering lengths across the periodic table and between isotopes. The scattering length density (SLD) of a material is calculated using equation (2) where N is the number density of atoms in a material and b_i is the scattering length of each nucleus.

$$\rho = \sum Nb_i \quad (2)$$

The isotope effect is most clearly seen by the very different SLDs of H_2O and D_2O, $-0.56 \times 10^{-6} Å^{-2}$ and 6.35×10^{-6} $Å^{-2}$, respectively. Using isotopic substitution it is possible to study different reflectivity profiles in the same chemical environment. In this work, we have measured reflectivity profiles of the calcite/alginate solution in H_2O, D_2O, and a mixture of the two to form a solution that has the same scattering length density of the calcite crystal (4.69×10^{-6} $Å^{-2}$). This combination of solution contrasts is important to constrain the structural model. By using a solution with the same SLD as the calcite, a reflected signal is only seen from the adsorbed alginate (alginate SLD = 2.6×10^{-6} $Å^{-2}$, calculated from the expected molecular formula and specific gravity).

The measured reflectivity profile is then analysed by comparison of the experimental data with a model structure. The general approach is to constrain the structural model as much as possible to fit the data. If a single layer is found not be sufficient to fit the experimental data, adsorbed layers can be broken into several smaller blocks/layers to describe adsorbed structures in more detail. In some cases a mathematical description of the SLD profile is appropriate, such as exponential or Gaussian [32]. In all of these cases, the total reflected intensity from adsorbed layers is calculated using the matrix method developed by Abeles and used in reflectivity fitting programs such as RasCAL [33].

The polymer segment density distribution normal to the surface was modelled in several ways, discrete layers, exponential decrease from the surface, or a Gaussian distribution. The best fit to the data in all cases was found using the Gaussian distribution model. The SLD profile through the interface was modelled by dividing a 300 Å region into 10 Å sections with an interlayer rough-

ness fixed to 5 Å to smooth out each interface. The volume fraction of alginate was then calculated in each section and converted to an SLD by assuming the rest of the layer was filled with the subphase water. In all adsorbed alginate datasets it was observed that the volume fraction of alginate had reached background well before the model cut off at 300 Å except for the 2.5 ppm MVG where the model had to be extended to 350 Å to reach background. Using the modelled volume fraction distribution, an adsorbed amount was obtained from the area under the Gaussian polymer segment density distribution curve. Although it was possible to fit a small variation in the Gaussian profile, in all cases the distribution was found to conserve the area under the curve, within error, providing a good test of the robustness of the values for adsorbed amount. Errors were calculated using the bootstrap error analysis in the RasCAL program, where random parameter values are generated and a fit performed 100 times to generate confidence intervals. The parameter errors were then used to calculate the error in adsorbed amount, assuming the maximum and minimum possible values. The SLDs of substrate, subphase, and adsorbate were fixed, where possible, according to the literature values (Table S1). During the experiment it was noted that there was incomplete exchange of the liquids within the cells as the SLD of the H_2O subphase could not be fitted to the literature value, but rather a mixture of H_2O containing some D_2O, only when the liquid in the cell was exchanged from D_2O to H_2O in situ (despite repeated exchanges). This may be due to insufficient mixing of the two liquids from the density difference in the cell and the high contact angle between the water and the hydrophobic surface of the Teflon trough.

3. Results

Fig. 2 presents bulk solution depletion isotherms for the adsorption of MVM (green circles) and MVG (purple squares) to calcium carbonate powder. It can be seen that there is a small difference between the two alginate solutions with MVG adsorbing more to the surface than MVM. At low concentrations, all alginate is adsorbed as seen from a steep initial increase in adsorbed amount before the turning point of the isotherm at an equilibrium concentrations of roughly 2.5 ppm. At higher concentrations, the slope becomes shallower but not flat suggesting that the adsorption does not form a monolayer at the surface. There may be some precipitation of the alginate at higher concentrations as the calcium is dissolved into solution forming insoluble calcium alginate. The

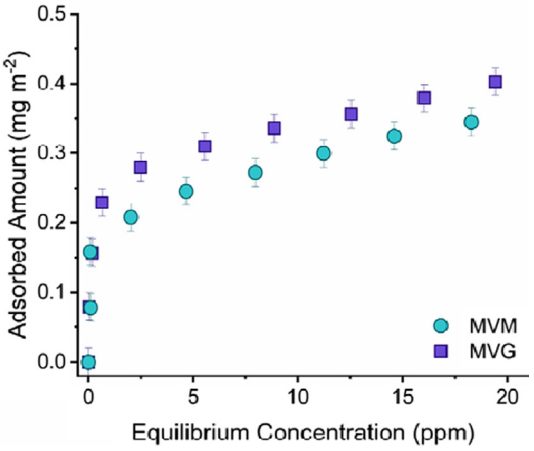

Fig. 2. Isotherm data of sodium alginate adsorption to calcite powder in water as measured by total organic carbon analysis (TOC). MVM alginate is shown as green circles and MVG as purple squares. (For interpretation of the references to colour in this figure legend, the reader is referred to the web version of this article.)

interaction between the calcium carbonate surface and alginate is observed to be weak due to the low adsorbed amount at equilibrium. This effect could be accentuated by the sample preparation for TOC analysis. In order to remove calcium carbonate powder from the supernatant, the samples are centrifuged at 15,000 G for 20 min which is likely to shear off any loosely bound alginate from the surface leaving only the tightly bound molecules that are effectively irreversibly adsorbed by attachment at multiple points.

3.1. Neutron reflection

Each calcite crystal was first measured in three saturated calcium carbonate water contrasts, D_2O, H_2O, and water contrast matched to calcite (CMC = 4.69×10^{-6} Å^{-2}). A representative dataset is shown in the supporting information (Fig. S2). Previous experiments have shown that the surface roughness of calcite does not increase over time in the presence of water saturated with calcium carbonate powder [27]. The surface cleanliness was confirmed by the absence of any reflected signal above the background level in the CMC contrast (not shown). Measuring the reflectivity in contrast matched water is especially useful due to the high sensitivity to adsorbed layers at the surface. Unlike silicon crystals, which have a surface oxide layer and always show a signal in contrast matched water, if the surface of calcite is completely clean there will be no signal recorded. The two (D_2O and H_2O) data sets were fitted simultaneously using only two fitting variables, surface roughness and H_2O contrast. All bare calcite crystals for the study were successfully fitted to a single interface model and the surface roughness varied from 8.5 ± 0.6 Å to 9.4 ± 0.3 Å.

Before adsorption measurements using neutron reflection it is important to completely characterise the surface that the adsorbate will bind to. Unlike many other surfaces used in reflection the calcite surface can be dynamic and of biogenic origin. Measurements of the bare surface are therefore useful to assess the cleanliness of the substrate and provide an initial roughness characterisation. When calcite is cleaved or polished, high-energy bonding sites are exposed. In air, these sites are likely to be contaminated with species from the atmosphere, however, this bonding of contaminants is generally weak and upon immersion, water molecules compete, removing the contaminants and hydrating the surface with pH sensitive groups [11,26,34].

3.2. Alginate adsorption

Fig. 3 presents experimental neutron reflectivity data of the calcite/water interface in the presence of (a) 2.5 ppm MVM and (b) 2.5 ppm MVG alginate in three contrasts, D_2O (purple squares), H_2O (green circles), and water contrast matched to calcite (CMC, yellow triangles). Corresponding SLD profiles are provided in the supporting information (Fig. S3). Alginate solutions were introduced to the sample cells at concentrations of 0.5 and 1 ppm in D_2O. Three water contrasts were recorded for the highest concentration, 2.5 ppm. The concentration of 2.5 ppm was chosen to be just above the turning point of the plateau for both MVM and MVG alginates in solution depletion isotherms (Fig. 2). This represents concentration where the surface is expected to be covered but before the onset of multilayer formation or precipitation.

Upon introduction of alginate the intensity of the reflectivity in both the H_2O and D_2O contrasts drop, suggesting that the surface is roughening and/or a diffuse layer is adsorbed. A signal is also seen in the contrast matched water indicating an adsorbed layer was present at the surface. This signal in the contrast matched water is purely from any adsorbed material at the interface and therefore has a rather low signal-to-noise ratio and large error bars. The 2.5 ppm MVM data was fitted to a Gaussian layer model with an adsorbed amount of 1.6 ± 0.4 mg m^2 and a surface roughness of 16.1 ± 0.9 Å. The volume fraction of alginate at the surface was

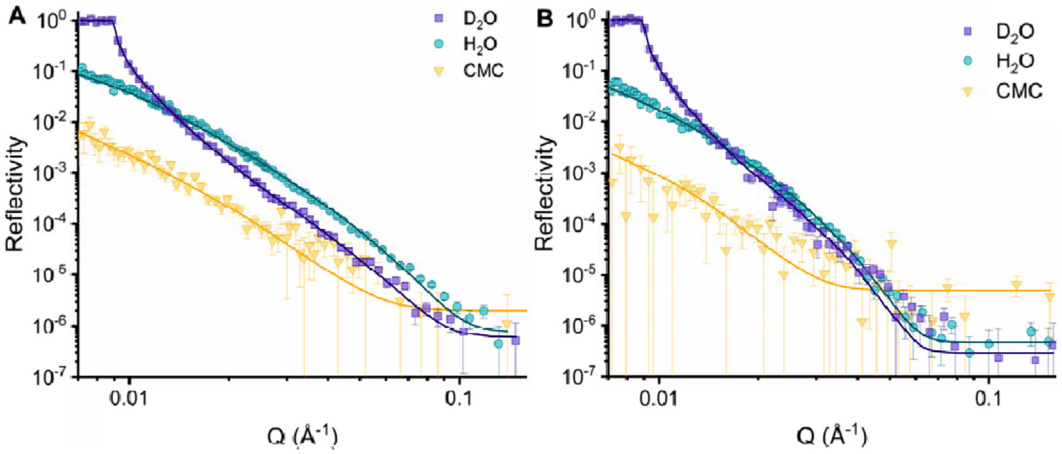

Fig. 3. Experimental neutron reflectivity data of the calcite/water interface in the presence of **A** 2.5 ppm MVM and **B** 2.5 ppm MVG alginate in three contrasts, D_2O (purple squares), H_2O (green circles) and water contrast matched to calcite (CMC, yellow triangles). Calculated fits to the data are overlaid as solid lines. (For interpretation of the references to colour in this figure legend, the reader is referred to the web version of this article.)

found to be 0.098 showing that the adsorbed layer is highly hydrated at the interface. The volume fraction decreases away from the surface into solution before reaching zero between 200 and 250 Å. As the concentration of MVM alginate increases, the amount adsorbed at the surface initially increases and begins to level off reaching 1.6 ± 0.4 mg m^2 at 2.5 ppm MVM. The SLD of the subphase in the H_2O was fitted to be higher (2.28 ± 0.05 × 10^{-6} $Å^{-2}$) than the literature value of −0.56 × 10^{-6} $Å^{-2}$, due to incomplete exchange, as discussed above. Table 1 shows the surface roughness and adsorbed amounts obtained from each fit to the Gaussian model described above.

Fig. 3b shows the experimental data measured for 2.5 ppm MVG in all three water contrasts. The data was fitted to a Gaussian layer model, as above, and again found to give good agreement in all datasets. The SLD of the H_2O contrast was again found to be higher than literature (3.28 ± 0.07 × 10^{-6} $Å^{-2}$) as for MVM alginate. The polymer distribution was found to extend further into solution compared to MVM, suggesting that the MVG molecule is less attracted to the calcite surface. This may also be related to a greater degree of cross-linking by calcium ions compared to MVM alginate [17]. The modelled roughness, 34.5 ± 0.7 Å, is large and the reflected signal (above the critical edge) was much lower than for other measurements and reached background at lower Q. The larger roughness indicates more calcium is released into the solution to achieve equilibrium when compared to MVM alginate. The amount adsorbed with concentration follows a similar profile as the MVM alginate; however, the value at 2.5 ppm is higher (2.8 ± 0.3 mg m^2) showing that more alginate is adsorbed when the polymer contains higher ratios of guluronate residues.

3.3. High guluornate alginate with magnesium

The reflectivity study of the MVG alginate adsorption to calcite in pure water indicated significant surface roughening, attributed here to sequestration of calcium by the alginate molecule. It is not possible to pre-saturate the water with calcium ions due to the insolubility of calcium alginate and hence transport of calcium alginate to the calcite surface for adsorption would be impossible. By adding 12 mM $MgCl_2$ (same concentration of calcium in saturated $CaCO_3$ water) and allowing the system to equilibrate, the magnesium ions bind non-specifically with the alginate, reducing the effective charge of the polymer, making it less likely to be attracted to the calcite surface [23]. The affinity of magnesium compared to calcium is thought to be similar for MM and MG blocks but considerably smaller for GG blocks where specific interactions with calcium prevail. As the alginates used in the study contain a mixture of all blocks, we expect that the number of calcium ions removed from the surface will be lowered by the presence of magnesium and therefore less roughening of the calcite surface upon introduction to the sample cell. Magnesium ions have also been shown to bind to high energy sites on the calcite surface inhibiting dissolution [35].

Fig. 4 shows the fitted reflectivity data upon introduction of 2.5 ppm MVG pre-equilibrated with 12 mM $MgCl_2$ in D_2O (purple circles) and H_2O (green circles). The corresponding SLD profile is provided in the supporting information (Fig. S3). It was not possible to measure the CMC contrast due to time constraints of the experiment. The reflectivity profile shows a weak Kiessig fringe at higher Q suggesting a more defined adsorbed layer. Upon fitting the datasets, the maximum of the Gaussian polymer distribution is found to lie away from the calcite surface (Fig. 5a) and the adsorbed amount is lower than for MVG in pure water (0.7 ± 0.3 compared to 2.8 ± 0.3 mg m^{-2}). The surface roughness was also found to be lower 27.3 ± 0.5 Å compared to 34.5 ± 0.7 Å. The reduction in surface roughness by pre-saturation of the MVG with 12 mM $MgCl_2$ was not as pronounced as expected, suggesting that the affinity of MVG alginate for calcium ions is high even if the charge is compensated by other divalent ions. The composition of

Table 1
Values for roughness and adsorbed amount obtained from fits to the data of the adsorption to the calcite surface of sodium alginate in pure water.

Alginate Used	Parameter	Bare surface	0.5 ppm	1 ppm	2.5 ppm
MVM	Surface Roughness (Å)	9.4 ± 0.3	9.4 ± 1.1	10.6 ± 2.0	16.1 ± 0.9
	Adsorbed amount (mg m^{-2})	–	1.0 ± 0.5	1.4 ± 0.1	1.6 ± 0.4
MVG	Surface Roughness (Å)	8.9 ± 0.4	12.5 ± 1.3	18.0 ± 1.4	34.5 ± 0.7
	Adsorbed amount (mg m^{-2})	–	1.7 ± 0.3	2.7 ± 0.2	2.8 ± 0.3
MVG + 12 mM $MgCl_2$	Surface Roughness (Å)	8.5 ± 0.6	–	–	27.3 ± 0.5
	Adsorbed amount (mg m^{-2})	–	–	–	0.7 ± 0.3

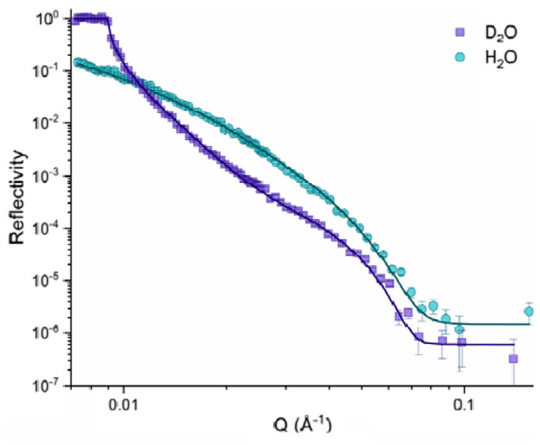

Fig. 4. Experimental neutron reflectivity data of the calcite/water interface in the presence of 2.5 ppm MVG pre-equilibrated with 12 mM $MgCl_2$ in two contrasts, D_2O (purple squares) and H_2O (green circles). Calculated fits to the data are overlaid as solid lines. (For interpretation of the references to colour in this figure legend, the reader is referred to the web version of this article.)

the alginate (i.e. the proportion and order of M to G residues) plays a greater role in the extent of calcite surface roughening than the availability of divalent ions in the solution.

3.4. Comparison

The data above shows the pronounced effect of the structural composition of sodium alginate on both the adsorption to and roughening of the surface of calcite crystals. Fig. 5 summarizes the differences observed in adsorbed amounts (Fig. 5b) and calcite surface roughness (Fig. 5c). As described above the adsorbed amount increases from zero but reached a plateau at higher concentrations. The surface roughness increases with concentration, suggesting that the sequestering of calcium ions to the alginate drives the surface dissolution of calcite. In the reflection experiments reported here we must carefully consider the solution and surface behaviour. Sodium alginate in the presence of calcium ions readily converts to calcium alginate, which has a very low solubility. In order to introduce the alginate to the sample cell without precipitation the reflectivity experiments must be run in pure water. However, the introduction of pure water to the calcite surface increases surface dissolution and roughening [26]. The technique of neutron reflection requires very flat surfaces for a good reflected signal and hence any dissolution should be kept to a minimum. However, we also exploit the sensitivity of the reflection to this roughening as an ideal way of probing the surface dissolution. In previous studies, calcite in contact with pure water was found to roughen quickly before plateauing at a roughness 2 nm greater than the original surface [26,36].

4. Discussion

This work is able to report on significant differences in the adsorption and surface roughening between the two investigated alginates: the alginate with the higher proportion of guluronate residues (MVG) is found increase calcite dissolution and shows a higher adsorption to the calcite surface compared to the alginate with a lower proportion of guluronate (MVM). As discussed above,

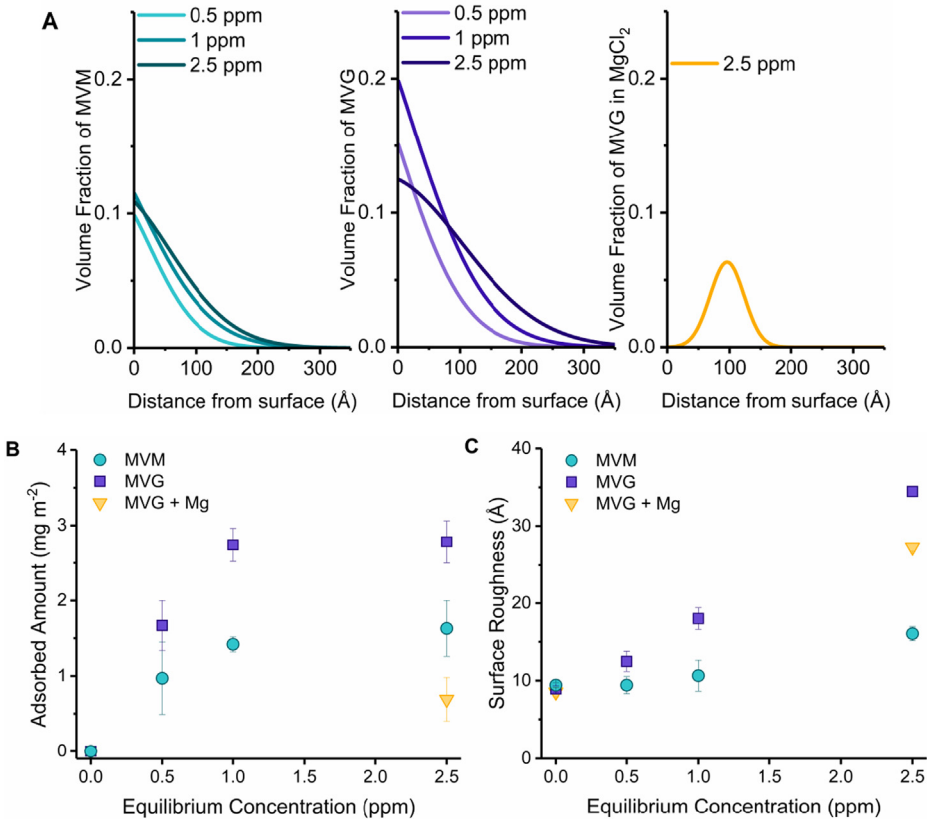

Fig. 5. Comparison of the fitted results obtained from neutron fitting from sodium alginate adsorption to calcite surfaces. Data from MVM are shown as green circles, MVG as purple squares and MVG pre-equilibrated with 12 mM $MgCl_2$ as yellow triangles. A. Gaussian distribution curves obtained from neutron reflection data fitting. B Adsorption isotherm of sodium alginate as calculated from the area under the curve of the Gaussian distribution of polymer adsorbed to the surface of calcite. C. Calcite surface roughness as a function of alginate concentration as obtained from neutron reflection fitting. (For interpretation of the references to colour in this figure legend, the reader is referred to the web version of this article.)

alginate in the presence of calcium is reported to crosslink preferentially between GG units causing gelation and insolubility known as the 'egg-box' model [17,21]. Therefore, the higher the proportion of G residues the higher affinity for the calcium either at the surface or in solution. However, the difference in M:G ratios between the two alginates is not large (46% vs. 69% guluronate residues) compared to the observed effects. The overall composition of the alginate does not tell us the sequence of sugar residues, which can consist of three different repeat unit sections, GG blocks, MM blocks or alternating MG blocks. The two alginates used in this study have not been tested for the proportion of each of these pair wise sections. Therefore, the MVG alginate may have a significantly higher proportion of the G residues in blocks of pure guluronate (i.e. GG) rather than in alternating MG sections. GG blocks are the most effective at crosslinking to form the 'egg box' structure that causes the molecule to become insoluble and inflexible. Furthermore, higher proportions of G blocks may favour polymer–polymer conformations rather than polymer-surface interactions and a more extended polymer conformation reaching out from the surface as we see for the 2.5 ppm MVG alginate where the polymer extends much farther out into solution as compared to MVM.

Addition of magnesium ions to the alginate solutions before introduction to the cell was found to reduce the alginate binding and surface roughness. This effect is probably due to lower effective charge of the alginate molecule by non-specific interactions with magnesium ions and lower binding of calcium leading to less ion removal from the calcite surface [22]. In addition, the pre-equilibrated alginate formed a different adsorption profile with the maximum adsorbed amount lying away from the surface as compared to that obtained from alginate adsorbed from pure water solutions where the maximum was found to lie at the surface of the calcite.

Polyelectrolyte adsorption to oppositely charged surfaces in low ionic strength solutions is complex and depends on a number of factors, including effective charge of the molecule due to specific ion binding, ionic strength, and surface charge [37,38]. At the interface, polyelectrolytes can form trains, loops, and tails, in differing ratios depending on the system of study. For lower polyelectrolyte charge densities, as would be expected for calcium saturated alginate in low salt conditions, loop and tail adsorption is favoured [37,39]. Entropic effects are also expected to play a major role in the adsorption of oppositely charged polyelectrolyte adsorption through the release of surface bound charge compensating counterions [40]. Also, in low ionic strength conditions the electrical double layer would extend far enough to trap molecules electrostatically.

There is a large body of work attempting to describe the interactions between alginate and calcium and its effect on calcium carbonate biomineralisation and dissolution. Experimental and theoretical treatments of the 'egg box' model have shown the process to occur via three stages during which mono, then bi-dentate binding is seen, before larger aggregations form, linked by calcium ions [15,41]. Borgogna *et. al.* reported that the specific binding of calcium ions to alginate occurs even at low concentration of calcium equilibrated with water [42]. The binding proceeds via a tilted egg-box model to minimise the repulsive interactions of the negative carboxylic acid groups. Experiments at the interface are more scarce, Perry *et. al.* studied the dissolution behaviour of calcite in the presence of alginate and reported that etch pits on the surface were lengthened along the obtuse angle of the rhombohedral pit due to bidentate binding of the high energy calcium at the edge of the pit to a GG dimer [43,44]. In these experiments, the proportion of guluronate residues is suggested to be the key to the increased interactions with calcium ions.

The present work agrees well with the solution and adsorption data from previous studies where the high guluronate alginate (MVG) both adsorbs more to the calcite surface and dissolves the surface to a greater extent than the same concentration of alginate with a lower guluronate content (MVM). By studying this complex system using neutron reflection we were able to study not only the adsorbed amount but also how the alginate adsorbed structure is affected by sugar chain composition and the addition of magnesium. We find that the adsorbed amount is greatly reduced when studying bulk isotherms that have been centrifuged, indicating that 90% of the adsorbed polymer in the static system is only weakly attached to the surface. We also find that higher concentrations of MVG, with and without magnesium ions, extend further out into solution (compared to low concentrations and low guluronate alginates) suggesting more loop and tail formation and less affinity for the calcite surface. These results can be used to understand the formation of highly charged polysaccharide coatings and hydrogels in the presence of divalent cations for biodegradable tissue scaffolds or injectable biomaterials [45–47]. Future studies in marine-like salt conditions as well as more complex extracellular matrix polysaccharides would build on this knowledge to understand how bacterial anchoring occurs to limestone rocks and soils.

5. Conclusion

Neutron reflectivity was able to demonstrate processes occurring during adsorption of alginate to calcite surfaces, of interest to studies of bacterial anchoring to limestone rocks and biomineralisation. The system is extremely complex in terms of adsorption, solution chemistry and ion complexation. However, by careful control of the solution composition we are able to identify that these polymers are observed to form thick, highly hydrated layers at the surface. The dissolution of the calcite crystal due to polymer complexation was significant and was followed on an Ångström scale without perturbing or removing the adsorbed molecules. The conformation of the 1,4-α linkage of the polysaccharide was found to alter the adsorbed amount and structure of the molecule at the interface. Alginate molecules containing high proportions of guluronate sugar residues adsorbed more and removed more calcium ions from the calcite surface when compared to alginate with a lower proportion of guluronate. This work shows the importance of polymer conformation and ion affinity on adsorption to dynamic dissolving calcite interfaces.

CRediT authorship contribution statement

Kathryn Louise Browning: Conceptualization, Methodology, Software, Investigation, Writing - original draft, Visualization. **Isabella N. Stocker:** Conceptualization, Methodology, Investigation, Writing - review & editing. **Philipp Gutfreund:** Software, Investigation, Resources, Data curation, Writing - review & editing. **Stuart Matthew Clarke:** Conceptualization, Methodology, Software, Investigation, Writing - review & editing, Supervision, Funding acquisition.

Declaration of Competing Interest

The authors declare that they have no known competing financial interests or personal relationships that could have appeared to influence the work reported in this paper.

Acknowledgments

We acknowledge the Partnership for Soft Condensed Matter (PSCM) for the use of the UV/ozone cleaner and the laboratory. We thank the Materials Characterisation Lab at the ISIS Neutron and Muon Source, UK, for use of the x-ray reflectometer and Liv Sofia Elinor Damgaard for help with the XRR data. We thank the ILL for the beam time to study this system (experiment number: 9-10-1140). Martin Malmsten is gratefully acknowledged for help-

ful discussions during the manuscript preparation. We would like to thank BP Plc. (KLB and INS) and Leo Foundation (Grant No. 2016-11-01, KLB) for funding.

Appendix A. Supplementary data

Supplementary data to this article can be found online at https://doi.org/10.1016/j.jcis.2020.07.088.

References

[1] A. Hernández-Hernández, M.L. Vidal, J. Gómez-Morales, A.B. Rodríguez-Navarro, V. Labas, J. Gautron, Y. Nys, J.M. García Ruiz, Influence of Eggshell Matrix Proteins on the Precipitation of Calcium Carbonate (CaCO3), J. Cryst. Growth 310 (7–9) (2008) 1754–1759, https://doi.org/10.1016/j.jcrysgro.2007.11.170.

[2] F.C. Meldrum, Calcium carbonate in biomineralisation and biomimetic chemistry, Int. Mater. Rev. 48 (3) (2003) 187–224, https://doi.org/10.1179/095066003225005836.

[3] S. Mann, The chemistry of form, Angew. Chemie 39 (19) (2000) 3392–3406, https://doi.org/10.1002/1521-3773(20001002)39:19<3392::aid-anie3392>3.0.co;2-m.

[4] L. Addadi, S. Raz, S. Weiner, Taking advantage of disorder: amorphous calcium carbonate and its roles in biomineralization, Adv. Mater. 15 (12) (2003) 959–970, https://doi.org/10.1002/adma.200300381.

[5] S.E. Wolf, I. Lieberwirth, F. Natalio, J.F. Bardeau, N. Delorme, F. Emmerling, R. Barrea, M. Kappl, F. Marin, Merging Models of Biomineralisation with Concepts of Nonclassical Crystallisation: Is a Liquid Amorphous Precursor Involved in the Formation of the Prismatic Layer of the Mediterranean Fan Mussel Pinna Nobilis?, Faraday Discuss. 159 (2012) 433–448, https://doi.org/10.1039/c2fd20045g.

[6] A.W. Xu, Y. Ma, H. Cölfen, Biomimetic Mineralization, J. Mater. Chem. 17 (5) (2007) 415–449, https://doi.org/10.1039/b611918m.

[7] J.L. Arias, M.S. Fernández, Polysaccharides and Proteoglycans In Calcium Carbonate-Based Biomineralization, Chem. Rev. 108 (11) (2008) 4475–4482, https://doi.org/10.1021/cr078269p.

[8] M. Yang, S.L.S. Stipp, J. Harding, Biological control on calcite crystallization by polysaccharides, Cryst. Growth Des. 8 (11) (2008) 4066–4074, https://doi.org/10.1021/cg800508t.

[9] F.C. Meldrum, R.P. Sear, Now you see them, Science (80-) 322 (5909) (2008) 1802–1803, https://doi.org/10.1126/science.1167221.

[10] W.M. Haynes, CRC Handbook of Chemistry and Physics: A Ready-Reference Book of Chemical and Physical Data, CRC Press, 2011.

[11] W. Stumm, J.J. Morgan, Aquatic Chemistry An Introduction Emphasizing Chemical Equilibria in Natural Waters, Wiley, 1981.

[12] M.F. Butler, N. Glaser, A.C. Weaver, M. Kirkland, M. Heppenstall-Butler, Calcium Carbonate Crystallization in the Presence of Biopolymers, Cryst. Growth Des. 6 (3) (2006) 781–794, https://doi.org/10.1021/cg050436w.

[13] B. Vu, M. Chen, R. Crawford, E. Ivanova, Bacterial Extracellular Polysaccharides Involved in Biofilm Formation, Molecules 14 (7) (2009) 2535–2554, https://doi.org/10.3390/molecules14072535.

[14] A.W. Decho, Overview of Biopolymer-Induced Mineralization: What Goes on in Biofilms?, Ecol. Eng. 36 (2) (2010) 137–144, https://doi.org/10.1016/j.ecoleng.2009.01.003.

[15] Y. Fang, S. Al-Assaf, G.O. Phillips, K. Nishinari, T. Funami, P.A. Williams, A. Li, Multiple Steps and Critical Behaviors of the Binding of Calcium to Alginate, J. Phys. Chem. B 111 (10) (2007) 2456–2462, https://doi.org/10.1021/jp0689870.

[16] W. Sabra, A.P. Zeng, W.D. Deckwer, Bacterial Alginate: Physiology, Product Quality and Process Aspects, Applied Microbiology and Biotechnology. (2001) 315–325, https://doi.org/10.1007/s002530100699.

[17] O. Smidsrød, Molecular Basis for Some Physical Properties of Alginates in the Gel State, Faraday Discuss. Chem. Soc. 57 (1974) 263–274, https://doi.org/10.1039/DC9745700263.

[18] I. Donati, S. Holtan, Y.A. Mørch, M. Borgogna, M. Dentini, G. Skjåk-Bræk, New Hypothesis on the Role of Alternating Sequences in Calcium-Alginate Gels, Biomacromolecules 6 (2) (2005) 1031–1040, https://doi.org/10.1021/bm049306e.

[19] A. Haug, S. Myklestad, B. Larsen, O. Smidsrød, G. Eriksson, R. Blinc, S. Paušak, L. Ehrenberg, J. Dumanović, Correlation between Chemical Structure and Physical Properties of Alginates, Acta Chem. Scand. 21 (1967) 768–778, https://doi.org/10.3891/acta.chem.scand.21-0768.

[20] P. Gacesa, Alginates, Carbohydr. Polym. 8 (3) (1988) 161–182, https://doi.org/10.1016/0144-8617(88)90001-X.

[21] G.T. Grant, E.R. Morris, D.A. Rees, P.J.C. Smith, D. Thom, Biological Interactions between Polysaccharides and Divalent Cations: The Egg-Box Model, FEBS Lett. 32 (1) (1973) 195–198, https://doi.org/10.1016/0014-5793(73)80770-7.

[22] I. Donati, A. Cesàro, S. Paoletti, Specific Interactions versus Counterion Condensation. 1. Nongelling Ions/Polyuronate Systems, Biomacromolecules 7 (1) (2006) 281–287, https://doi.org/10.1021/bm050646p.

[23] I. Donati, F. Asaron, S. Paoletti, Experimental Evidence of Counterion Affinity in Alginates: The Case of Nongelling Ion Mg2+, J. Phys. Chem. B 113 (39) (2009) 12877–12886, https://doi.org/10.1021/jp902912m.

[24] I. Donati, J.C. Benegas, A. Cesàro, S. Paoletti, Specific Interactions versus Counterion Condensation. 2. Theoretical Treatment within the Counterion Condensation Theory, Biomacromolecules 7 (5) (2006) 1587–1596, https://doi.org/10.1021/bm050981d.

[25] J. Penfold, R.K. Thomas, The Application of the Specular Reflection of Neutrons to the Study of Surfaces and Interfaces, *Journal of Physics: Condensed Matter*. IOP Publishing (1990) 1369–1412, https://doi.org/10.1088/0953-8984/2/6/001.

[26] I.N. Stocker, K.L. Miller, S.Y. Lee, R.J.L. Welbourn, A.R. Mannion, I.R. Collins, K.J. Webb, A. Wildes, C.J. Kinane, S.M. Clarke, Neutron Reflection at the Calcite-Liquid Interface, Berlin, Heidelberg 139 (2012) 91–99, https://doi.org/10.1007/978-3-642-28974-3_16.

[27] N. Stocker, I.; L. Miller, K.; Y. Lee, S.; R. Collins, I.; M. Clarke, S.; J. Webb, K.; J. Kinane, C.; Wildes, A. Adsorption at the Calcite – Liquid Interface with Molecular Precision. In IOR 2011 - 16th European Symposium on Improved Oil Recovery; EAGE Publications BV, 2014. https://doi.org/10.3997/2214-4609.201404793.

[28] I.N. Stocker, K.L. Miller, R.J.L. Welbourn, S.M. Clarke, I.R. Collins, C. Kinane, P. Gutfreund, Adsorption of Aerosol-OT at the Calcite/Water Interface - Comparison of the Sodium and Calcium Salts, J. Colloid Interface Sci. 418 (2014) 140–146, https://doi.org/10.1016/j.jcis.2013.11.046.

[29] T. Saerbeck, R. Cubitt, A. Wildes, G. Manzin, K.H. Andersen, P. Gutfreund, Recent Upgrades of the Neutron Reflectometer D17 at ILL, J. Appl. Crystallogr. 51 (2) (2018) 249–256, https://doi.org/10.1107/S160057671800239X.

[30] P. Gutfreund, T. Saerbeck, M.A. Gonzalez, E. Pellegrini, M. Laver, C. Dewhurst, R. Cubitt, Towards Generalized Data Reduction on a Chopperbased Time-of-Flight Neutron Reflectometer, J. Appl. Crystallogr. 51 (3) (2018) 606–615, https://doi.org/10.1107/S160057671800448X.

[31] Sivia, D. S. Elementary Scattering Theory; Oxford University Press, 2013. https://doi.org/10.1093/acprof:oso/9780199228676.001.0001.

[32] T. Cosgrove, Volume-Fraction Profiles of Adsorbed Polymers, J. Chem. Soc. Faraday Trans. 86 (9) (1990) 1323–1332, https://doi.org/10.1039/FT9908601323.

[33] RasCAL download | SourceForge.net https://sourceforge.net/projects/rscl/ (accessed Feb 20, 2020).

[34] Madsen, L. Calcite: Surface Charge. In Encyclopedia of Surface and Colloid Science, Third Edition; Somasundaran, P., Ed.; Taylor & Francis Group: New York, 2006; pp 1084–1096. https://doi.org/10.1081/E-ESCS3-120000648.

[35] R.G. Compton, C.A. Brown, Inhibition of Calcite Dissolution/Precipitation: Mg2 + Cations, J. Colloid Interface Sci. 165 (2) (1994) 445–449, https://doi.org/10.1006/jcis.1994.1248.

[36] J. Bisschop, D.K. Dysthe, C.V. Putnis, B. Jamtveit, In Situ AFM Study of the Dissolution and Recrystallization Behaviour of Polished and Stressed Calcite Surfaces, Geochim. Cosmochim. Acta 70 (7) (2006) 1728–1738, https://doi.org/10.1016/j.gca.2005.12.013.

[37] G. Fleer J.M.H.M. Scheutjens, T. Cosgrove and B. Vincent, M. A. C. S. Polymer at Interfaces; Springer Netherlands, 1998. https://doi.org/https://www.springer.com/gp/book/9780412581601.

[38] M. Kawaguchi, A. Takahashi, Polymer Adsorption at Solid-Liquid Interfaces, Adv. Colloid Interface Sci. 37 (3–4) (1992) 219–317, https://doi.org/10.1016/0001-8686(92)80085-C.

[39] E.M. Lee, R.K. Thomas, A.R. Rennie, Reflection of Neutrons from a Polymer Layer Adsorbed at the Quartz-Water Interface, EPL 13 (2) (1990) 135–141, https://doi.org/10.1209/0295-5075/13/2/007.

[40] V. Klitzing, R. Internal Structure of Polyelectrolyte Multilayer Assemblies. Physical Chemistry Chemical Physics. The Royal Society of Chemistry November 8, 2006, pp 5012–5033. https://doi.org/10.1039/b607760a.

[41] I. Braccini, S. Pérez, Molecular Basis of Ca2+-Induced Gelation in Alginates and Pectins: The Egg-Box Model Revisited, Biomacromolecules 2 (4) (2001) 1089–1096, https://doi.org/10.1021/bm010008g.

[42] M. Borgogna, G. Skjåk-Bræk, S. Paoletti, I. Donati, On the Initial Binding of Alginate by Calcium Ions. The Tilted Egg-Box Hypothesis, J. Phys. Chem. B 117 (24) (2013) 7277–7282, https://doi.org/10.1021/jp4030766.

[43] T.D. Perry IV, O.W. Duckworth, C.J. McNamara, S.T. Martin, R. Mitchell, Effects of the Biologically Produced Polymer Alginic Acid on Macroscopic and Microscopic Calcite Dissolution Rates, Environ. Sci. Technol. 38 (11) (2004) 3040–3046, https://doi.org/10.1021/es035299a.

[44] Perry; Duckworth, O. W.; Kendall, T. A.; Martin, S. T.; Mitchell, R. Chelating Ligand Alters the Microscopic Mechanism of Mineral Dissolution. J. Am. Chem. Soc. 2005, 127 (16), 5744–5745. https://doi.org/10.1021/ja042737k.

[45] T.E.L. Douglas, K. Sobczyk, A. Łapa, K. Włodarczyk, G. Brackman, I. Vidiasheva, K. Reczyńska, K. Pietryga, D. Schaubroeck, V. Bliznuk, et al., Ca:Mg:Zn:CO 3 and Ca:Mg:CO 3-Tri-and Bi-Elemental Carbonate Microparticles for Novel Injectable Self-Gelling Hydrogel-Microparticle Composites for Tissue Regeneration Related Content, Biomed. Mater. 12 (2) (2017), https://doi.org/10.1088/1748-605X/aa6200 025015.

[46] B. Ren, X. Chen, S. Du, Y. Ma, H. Chen, G. Yuan, J. Li, D. Xiong, H. Tan, Z. Ling, et al., Injectable Polysaccharide Hydrogel Embedded with Hydroxyapatite and Calcium Carbonate for Drug Delivery and Bone Tissue Engineering, Int. J. Biol. Macromol. 118 (2018) 1257–1266, https://doi.org/10.1016/j.ijbiomac.2018.06.200.

[47] M. Saveleva, A. Vladescu, C. Cotrut, L. Van Der Meeren, M. Surmeneva, R. Surmenev, B. Parakhonskiy, A.G. Skirtach, The Effect of Hybrid Coatings Based on Hydrogel, Biopolymer and Inorganic Components on the Corrosion Behavior of Titanium Bone Implants, J. Mater. Chem. B 7 (43) (2019) 6778–6788, https://doi.org/10.1039/c9tb01287g.